



Effect of tides on river water behavior over the eastern shelf seas of China

Lei Lin^{1,2}, Hao Liu¹, Xiaomeng Huang², Qingjun Fu¹, Xinyu Guo³

¹ College of Ocean Science and Engineering, Shandong University of Science and Technology, Qingdao 266590, China

5 ² Ministry of Education Key Laboratory for Earth System Modeling, Department of Earth System Science, Tsinghua University, Beijing 100084, China

³ Center for Marine Environmental Study, Ehime University, Matsuyama 790-8577, Japan

Correspondence to: Lei Lin (llin@sdust.edu.cn; linlei24@126.com)

Abstract. Rivers carry large amounts of freshwater and terrestrial material into shelf seas, which is an important part of the global water and biogeochemical cycles. The earth system model or climate model is an important instrument for simulating and projecting the global water cycle and climate change, in which tides however are commonly removed. For a better understanding of the potential effect of the absence of tides in the simulation of the water cycle, this study compared the results of a regional model with and without considering tides, and evaluated the effect of tides on the behavior of three major rivers (i.e., the Yellow, Yalujiang, and Changjiang Rivers) water in the eastern shelf seas of China from the perspectives of transport pathways, timescales, and water concentration. The results showed that the tides induced more dispersed transport for the water of the Yellow and Yalujiang rivers, but more concentrated transport for the Changjiang River water. The effect of tides on the transit areas of the Yellow, Yalujiang, and Changjiang Rivers was 13, 40, and 21 %, respectively. The annual mean water age and transit time of the three rivers in the model with tides were several (~2–10) times higher than those in the no-tide model, suggesting that tides dramatically slow the river water transport and export rate over the shelf. By slowing the river water export, tides induced a three-fold increase in river water concentration and a decrease in shelf seawater salinity by >1. Moreover, the effect of tides on river behavior was stronger in relatively enclosed seas (i.e., the Bohai and Yellow Seas) than in relatively open seas (i.e., the East China Sea). The change in the shelf currents induced by tides is the main cause of the difference in the river water behavior between the two model runs. Tides can increase bottom stress and thus weaken shelf currents and decrease the water transport timescales. The improvement in tidal parameterization in the no-tide model in the simulation of river water behavior was very limited. Given the important role of river runoff on the global water cycle and the effect of changes in river water behavior on ocean carbon cycling, it is important to include the tidal effect in earth system models to improve their projection accuracy.

1 Introduction

Rivers carry large amounts of freshwater and terrestrial material into shelf seas, which plays a crucial role in the global water cycle and the global biogeochemical cycle. For instance, on a global scale, river runoff contributes to about 10% of the



global meridional water fluxes, modulating the ocean circulation by affecting the water balance and salinity of the oceans (Oki et al., 1995; 1999). Approximately 400 Mt of organic carbon, 54 Mt of terrestrial nitrogen, and 8.5 Mt of phosphorus are annually discharged into the shelf seas by rivers (Mackenzie & Lerman, 2002; Schlünz & Schneider, 2000; Hopkinson & Vallino, 2005), which have an important impact on marine primary productivity and carbon cycling (Dittmar & Kattner, 2003; Gong et al., 2011). The continental shelf sea is the first stop for the river water to enter the ocean. As the shelf seas connect the rivers and deep oceans as well as are the most productive part of the world's oceans, the river water behavior over the shelf seas is critical for the processes of the global water and biogeochemical cycle.

Earth system models or climate models are important tools to represent and project the global water and biogeochemical cycles and climate change (e.g., Winkelbauer et al., 2022; Brady et al., 2019; Dufresne et al., 2013; Clark et al., 2015). An accurate simulation of the river water behavior over the shelf seas is one of key steps for accurate simulation in these models, but is usually hard to be achieved in earth system models or climate models (Feng et al., 2021). On one hand, climate models used relatively large grid cells which are too coarse for shelf seas with relatively small spatial scales (Graham et al., 2018; Feng et al., 2021; Holt et al., 2017). This issue would be addressed in the future as the computation power increase. On the other hand, climate models usually do not explicitly consider the tidal process since the tides have much shorter timescales than the ocean circulation and water cycle and could induce numerical instability of models (Lee et al., 2006; Luneva et al., 2015; Voltaire et al., 2013; Müller et al., 2010). However, tides are the major motions of shelf seawater and play a crucial role in hydrodynamic processes in shelf seas. A model without considering tides may induce a large bias in the simulation of the river water behavior. Thus, to better understand the potential consequences of the absence of tides in climate models, it is necessary to first quantitatively evaluate the impact of tides on the behavior of river water on the shelf.

Previous studies have suggested that tides can significantly influence shelf hydrodynamics and thus, river water behavior. For instance, Guo and Valle-Levinson (2007) found that tidal mixing intensifies the salinity gradient and restricts the upstream extension of the river plume off the Chesapeake Bay. Wu et al. (2011, 2014) pointed out that tidal forcing increases vertical mixing and results in a strong horizontal salinity gradient at the northern edge of the Changjiang River plume and restricts its northward extension, while the tide-induced Stokes drift along the coast facilitates the northward transport of the Changjiang River water to the Jiangsu coast. A numerical study by Liu et al. (2012) suggested that tidal forcing plays the most dominant role in controlling the age of the Yellow River water in the Bohai Sea. Further, Yu et al. (2021) found that upstream tide-induced residual currents induced the upstream transport of freshwater around the Yellow River mouth. All these studies demonstrate that tides can influence the current or mixing processes and thus, modulate river water behavior over the shelf. However, most of these studies have focused on the effect of tides on river water transport in estuaries and their adjacent seas, while few studies have evaluated the effect of tides on river water behavior at the spatial scale of the entire shelf sea.

The eastern shelf seas of China (ESSC) with energetic tides have wide continental shelves (Figure 1). The ESSC includes the Bohai, Yellow, and the East China Seas. It connects the rivers of China and the Korean Peninsula to the Western Pacific Ocean. Among these rivers, the Yellow, Yalujiang, and Changjiang Rivers are the three with the largest discharge. The



85 The remainder of this study is organized as follows: Section 2 introduces the models and diagnostic methods for river water
transport pathways, timescales, and concentration. Section 3 presents the results of the impact of tides on the water behavior
of the three rivers over the shelf. By analysing the change in the shelf circulation and the results of sensitivity experiments,
Section 4 discusses the dynamic mechanism on the tidal effect on the river water behavior. The potential effect of the
absence of tides on climate modelling are also discussed in Section 4. Finally, Section 5 provides a brief conclusion of the
90 study.

2 Models and Methods

2.1 Hydrodynamic Model

The hydrodynamic model used in this study was the Princeton Ocean Model (Blumberg and Mellor, 1987). The model for
ESSC was initially set up by Guo et al. (2003) and Wang et al. (2008). The model included the four major tidal constituents
95 and covered the entire ESSC (Figure 1). Its horizontal grid resolution was ~5-6 km. This study focused on the climatological
state results, and thus the model was driven by climatological mean forcings (Wang et al., 2008). The monthly mean river
runoff values of the Changjiang, Yellow, and Yalujiang Rivers (Table 1) were derived from measurements of river
hydrological stations and the marine atlas, were linearly interpolated to each time step during the model run. This model has
been successfully applied to simulation studies of riverine nutrient transport and cycling in the ESSC (Zhao and Guo, 2011;
100 Zhang et al., 2019; Wang et al., 2019; Zhang et al., 2021), the Yellow River age and plume in the Bohai Sea (Liu et al., 2012;
Yu et al., 2020), the Yellow Sea cold water mass (Zhu et al., 2018), and the water residence time of the shelf sea (Lin et al.,
2020). These studies have well validated the model and demonstrated the model reliability and applicability in the ESSC.
The readers are referred to Wang et al. (2008) and Guo et al. (2003) for more detailed descriptions. The hydrodynamic fields
from the hydrodynamic model, including the sea level, velocity, and diffusivity coefficients were used to drive the particle-
105 tracking and passive tracer models.

Table 1. The monthly mean river runoff (m³/s) of the Changjiang, Yellow, and Yalujiang Rivers in the hydrodynamic model.

Rivers	Jan.	Feb.	Mar.	Apr.	May.	Jun.	Jul.	Aug.	Sep.	Oct.	Nov.	Dec.
Changjiang	10834	12017	17171	25282	33188	39942	52840	44952	40323	32117	22136	13776
Yalujiang	656	657	709	693	695	828	1353	2117	1158	699	678	685
Yellow	378	296	299	209	216	271	907	1481	1345	1084	619	440



2.2 Particle-tracking and passive tracer models for diagnosing river water behaviour

110 In this study, the particle-tracking method used to obtain the trajectory of river water over the shelf is from the estuarine and
coastal ocean model coupled with a sediment transport module (ECOMSED) (Blumberg, 2002), which has been used in the
study of the Yellow River water transport in the Bohai Sea (Liu et al., 2012; Wang et al., 2013). In the numerical
experiments, we released 1000 particles at each of the three river boundaries at 0 o'clock every day and ran the particle-
tracking model for 30 years. The location of each particle and its time after release were recorded for the analysis of the
115 particle trajectory and calculation of the river water age.

To quantify the concentration of river water in the shelf seas, three passive tracers were released at the three river boundaries
with a dimensionless concentration of 1. Thus, the passive tracers of each river were equivalent to the freshwater
concentration, that is, the tracer concentration was 1 for freshwater and 0 for pure seawater. Tracer concentrations were
calculated using an offline advection-diffusion module from the Marine Environment Research and Forecasting model
120 (MERF) (Liu et al., 2016; Lin and Liu, 2019a; Tang et al., 2021), in which the TVDal and central-difference algorithms were
used in the discretization of the advection and diffusion terms, respectively (Lin and Liu, 2019b). The tracer model ran for
30 years and the results of the last year were outputted and analyzed.

2.3 Characterizing the pathway and transit area of river water

Based on the results of the particle-tracking model, the emergence probability of the particles at each grid over the shelf was
125 used to characterize the river water pathways and was calculated at $0.5^\circ \times 0.5^\circ$ grid cells by dividing the number of particles
emerging in the grid cell by the total number of particles released. A particle can re-enter a grid more than once, in which
case the same particle is counted only once for a given grid. In this way, we obtained the results of the emergence probability
for particles released on each day of one year. The annual mean emergence probability was used in the analysis of the river
water transport pathway, which was calculated by averaging the emergence probability on all days of the year. The main
130 water transport pathway is indicated by locations with high particle emergence probabilities.

Then, the transit area of the river water was calculated as the particles' emergence probability in each grid multiplied by the
area of the corresponding grid and summed over the shelf to quantify the magnitude of the influence range of the river on
shelf seas.

2.4 Transport timescales of river water

135 Water age and transit time were used to quantify the transport timescales of river water over the shelf.

2.4.1 Water age

Water age is defined as the time elapsed since a river water particle enters the domain of interest (Deleersnijder, 2001), and
can quantify the transport rate of the river water over the shelf. For a particle released at time t_0 , it moves to some position at



time t , and the water age at this position is $t-t_0$. Then, the mean water age for each grid cell was calculated using a weighted
140 average of all the particle ages at a grid cell at time t . Because the same number of particles was released every day, particles
released on different days denoted different water masses due to variation of the river discharge. Thus, the weighted average
of the mean water age was calculated using the river discharge on the particle release day as the weight coefficient. The
mean water age used in the analysis was calculated by averaging the particle age at $0.5^\circ \times 0.5^\circ$ grid cells. Due to space
limitations, this study only shows the annual mean of the vertical average results for the water age of the three rivers.

145 **2.4.2 Transit time**

The transit time of the river water over the shelf is defined as the time the river water particle spends from the river boundary
to the shelf boundary (red dashed lines in Figure 1), which can quantify the total retention time of the river water in the shelf
seas. A river particle released at time t_0 leaves the shelf at time t_1 , and its transit time, according to the definition is t_1-t_0 .

2.5 Sensitivity experiments

150 Numerical experiments were designed to explore the effect of tides on the river water fate in the ESSC, which were
conducted by using the model run with tides (hereafter termed ‘Control run’) and the model run without tides (hereafter
termed ‘No-Tide case’), respectively. In both experiments, the hydrodynamic model was run for three years, and the model
data output of the last year was used for analyzing and driving the particle-tracking and passive tracer models. Then, the
water transport pathways and timescales and the water concentrations of the rivers in the ESSC were determined using the
155 same procedures described in Sections 2.3 and 2.4.

3 Results

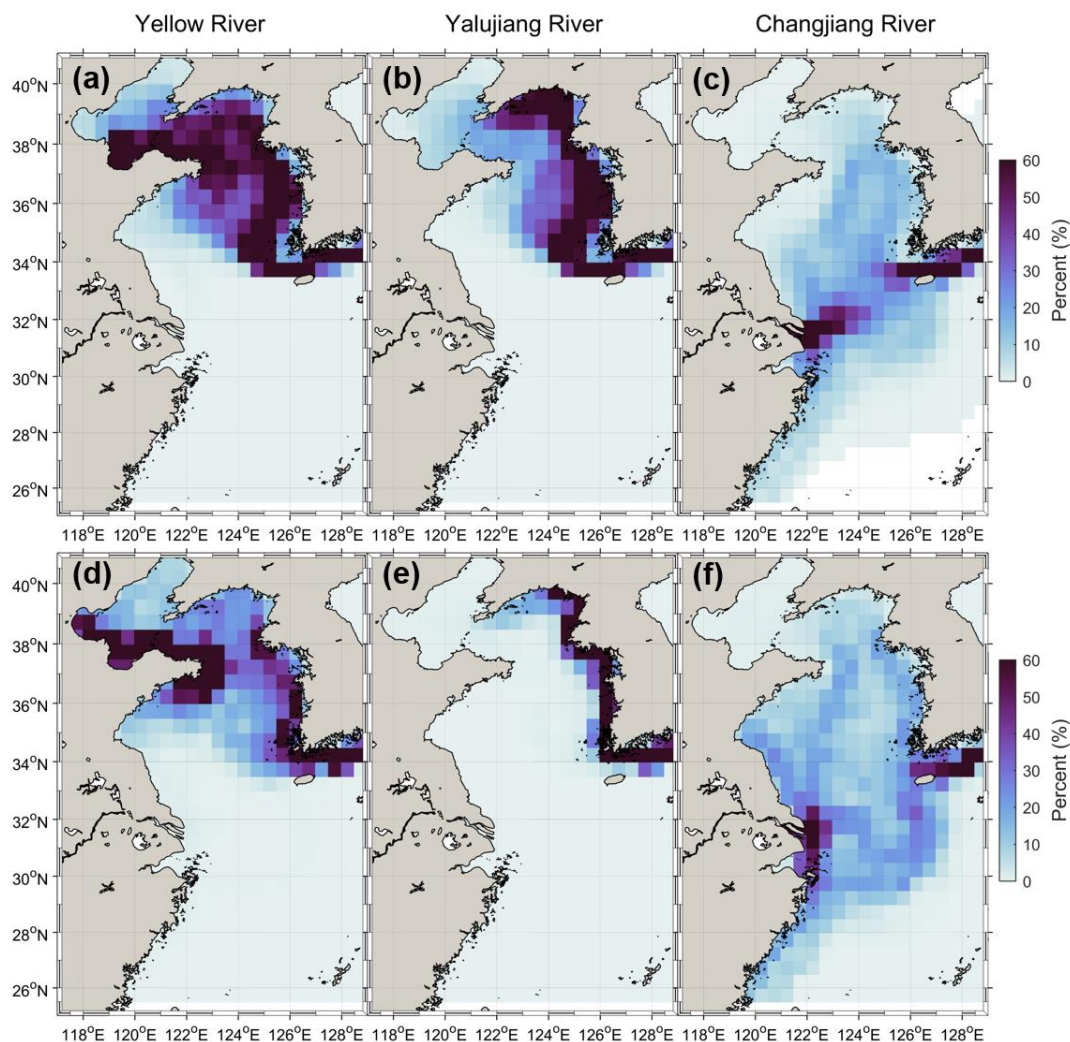
By comparing the model’s Control run and No-Tide case results, the effect of tides on the behavior of the three rivers’ waters
in the ESSC was analyzed for three aspects: the effect on river water transport pathways, transport timescales, and
concentrations.

160 **3.1 Effect on transport pathways**

Significant differences in the water transport pathways of the three rivers between the Control run and No-Tide case were
observed (Figure 2). As shown in the results of the Control run, most of the Yellow River water passes through the Bohai
Strait, enters the Yellow Sea, and finally leaves through the Cheju Strait (Figure 2a). This emergence probability suggests
that the Yellow River water passes through most of the Yellow Sea. The Yalujiang River water passes mainly through the
165 western Yellow Sea and leaves it through the Cheju Strait (Figure 2b). The Changjiang River water flows northeastward
after leaving the Changjiang estuary and leaves China’s eastern shelf through the Korea-Tsushima strait, with a probability



of ~10–20 % of it passing through the Yellow Sea (Figure 2c). The Changjiang River water is concentrated in the South Yellow Sea and north of the East China Sea.



170 **Figure 2.** The annually averaged emergence probability of the particles released at the three rivers' boundaries for the Control run (a–c) and No-Tide case (d–f), which are indicated by the emergence probability of the particles in the grids (in percent).

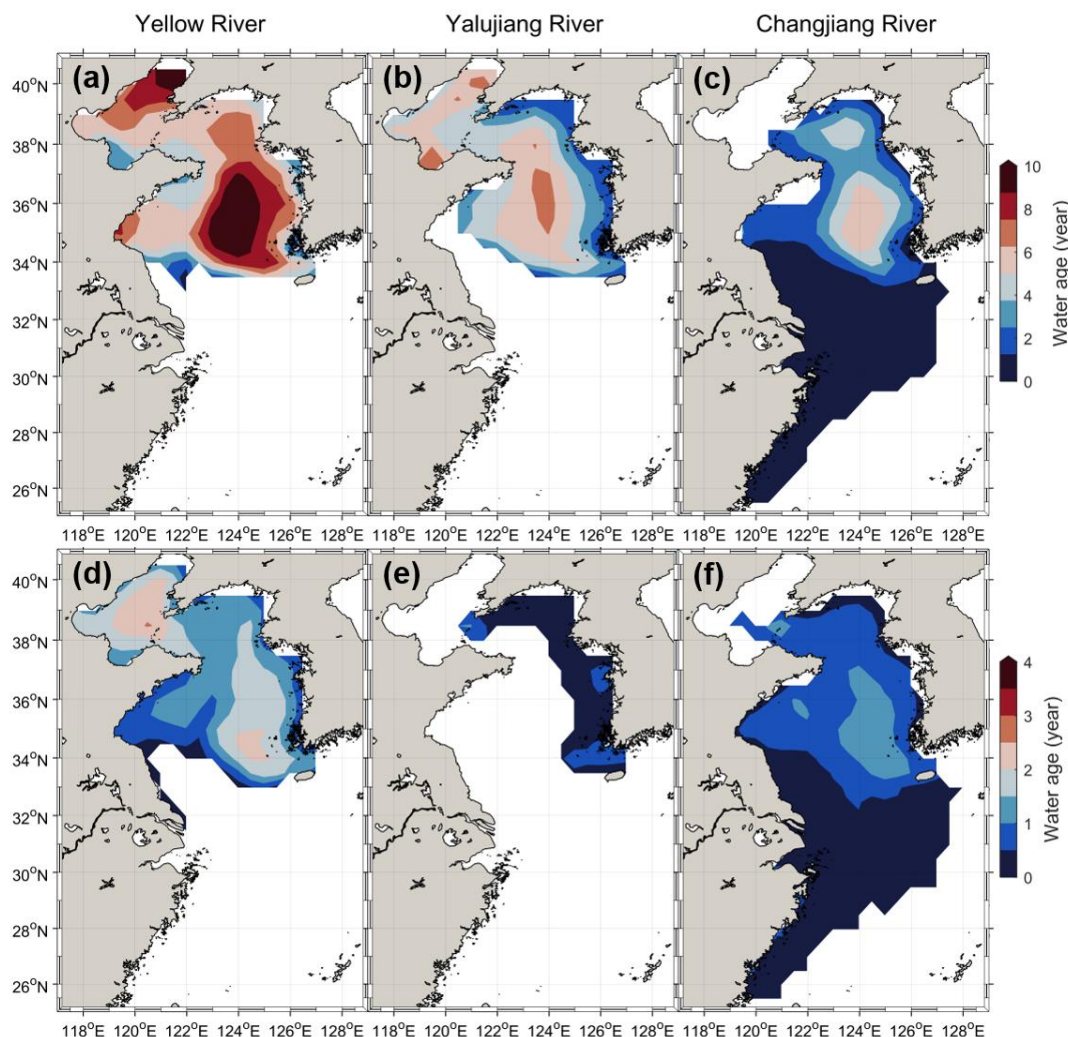
In comparison to the Control run, the water transport pathways of the Yellow River and Yalujiang River for the No-Tide case were more concentrated in the western coastal region of the Yellow Sea, as shown in the map of their emergence probability (Figures 2d and 2e). However, the emergence probability of the Changjiang River water for the No-Tide case increased in the Yellow Sea and East China Sea, particularly at the Jiangsu and Zhemu Coasts (Figure 2f). In comparison, the transit areas of the Yellow, Yalujiang, and Changjiang Rivers for the Control run are 2556, 2027, and 1537 km², respectively, while they are 2224, 1214, and 1851 km², respectively, for the No-Tide case. As compared with the control run,



180 the transit areas of the Yellow and Yalujiang Rivers for the No-Tide case decreased by 13 % and 40 %, respectively, while that of the Changjiang River increased by 21 %. The above results suggest that the tidal effect induced more dispersed transport for the Yellow and Yalujiang Rivers' waters but more concentrated transport for the Changjiang River water.

3.2 Effect on transport timescales

185 The transport timescales of the river water for the No-Tide case were significantly decreased as against the Control run. The water age for the three rivers showed high values (4–10 years) in the Bohai Sea and the Yellow Sea and much lower values (less than 1 year) in the East China Sea (Figures 3a–3c). The mean age of the Yellow and Yalujiang Rivers water was 4.7 and 4.5 years in the Bohai Sea and 5.5 and 3.1 years in the Yellow Sea, respectively. The water age of the Changjiang River in the Yellow and East China Seas was 1.3 and 0.3 years, respectively. Moreover, the relatively high water age of the three rivers is concentrated in the central Yellow Sea (123–126 E°, 34–39 N°), where the Yellow Sea Cold Water Mass (YSCWM) occurs every summer, suggesting that the YSCWM region could trap river water and terrigenous materials for several years. In comparison, when the tides were removed, the rivers' water age decreased significantly (Figures 3e–3f). For the No-Tide Case, the average age of the Yellow and Yalujiang Rivers water was 1.6 and 0.5 years in the Bohai Sea and 1.0 and 0.3 years in the Yellow Sea, respectively, and decreased by averagely more than 80 % as compared with the Control run. The mean water age of the Changjiang River in the Yellow Sea decreased to 0.5 years (by ~60 %) in the No-Tide case, while in the 195 East China Sea it remained basically unchanged. The dramatic decrease in the river water age for the No-Tide case suggests that the tides could significantly slow down the transport of river water over the shelf, especially in the relatively enclosed Yellow and Bohai Seas.



200 **Figure 3. The annually and vertically averaged water age of the three rivers for the Control run (a–c) and No-Tide case (d–f). Only results at locations with particle emergence probability of > 1 % have been presented.**

205 The shorter transport timescales of the rivers' waters for the No-Tide case are also shown in the transit time results (Figure 4). The annual mean transit time of the Yellow, Yalujiang, and Changjiang Rivers are 9.4, 5.6, and 2.2 years, respectively, while they decreased to 2.4, 0.4, and 1.2 years, respectively, in the No-Tide case. The apparent decrease in transit time indicated a much shorter retention in the shelf seas and a faster export rate of river water from the shelf seas for the No-Tide model than for the Control model considering tides. The mean transit time of the waters of the Yellow and Yalujiang Rivers for the No-Tide case decreased by 75 and 93 %, respectively, which are larger than that of the Changjiang River (45 %), suggesting that the effects of tides on the river water export rate could be more strong for rivers in relatively enclosed seas



than those in relatively open seas. Moreover, as against the Control run, the river water transit time for the No-Tide case
210 showed a different seasonal variation pattern and a decreased variance.

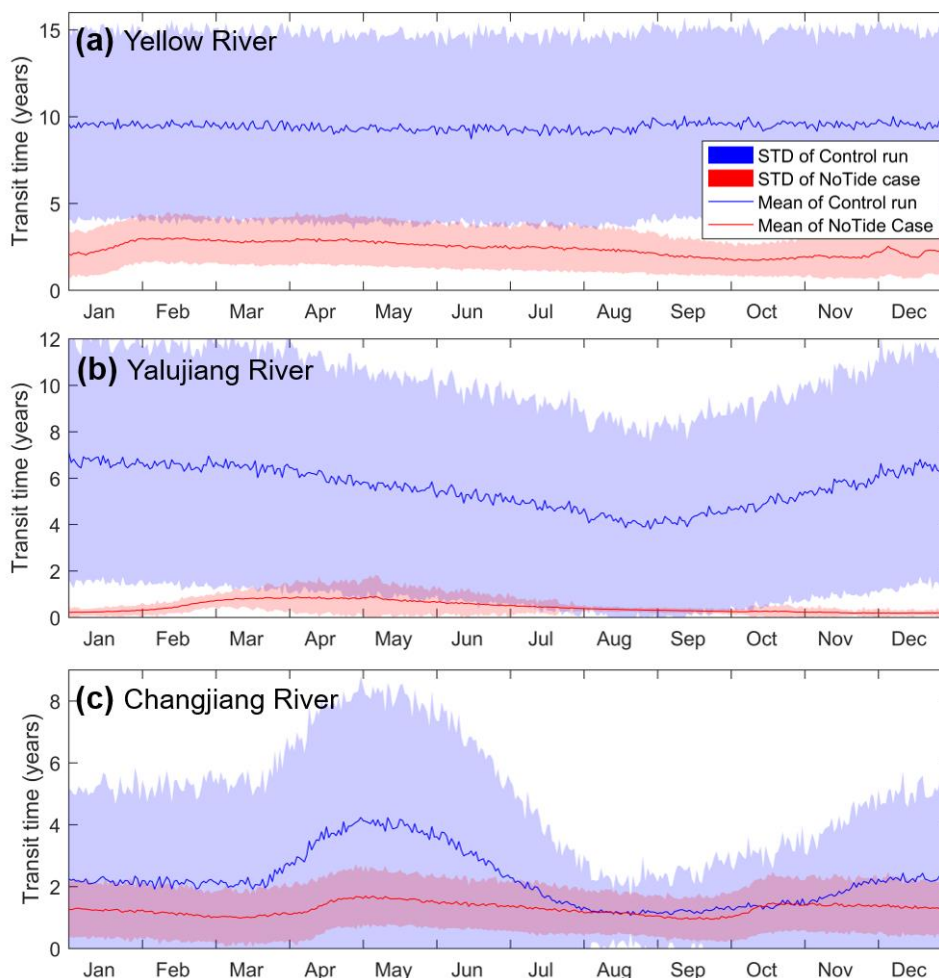
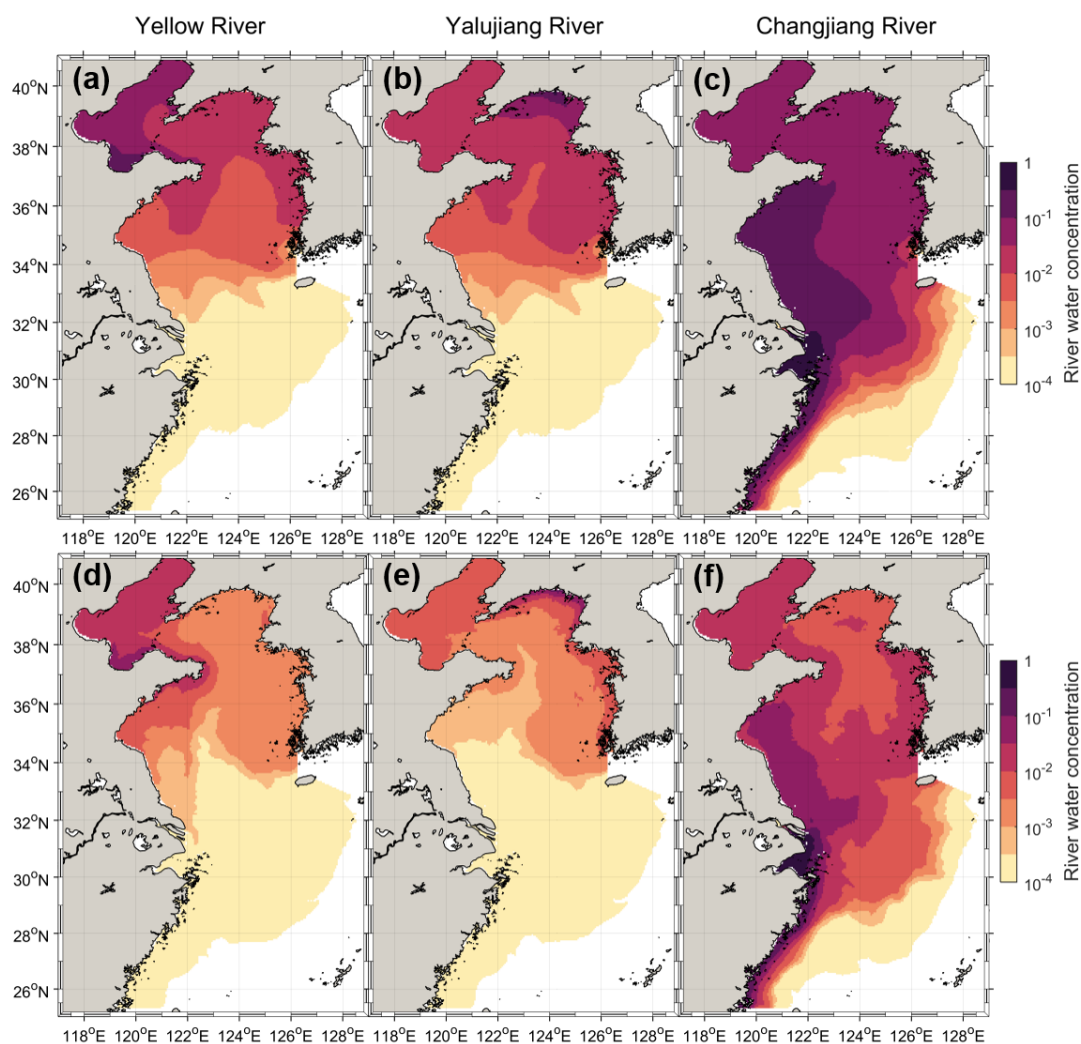


Figure 4. The daily mean water transit time over the shelf of the three rivers for the Control run (blue) and No-Tide case (red). STD in the figure label denotes the standard deviation of the transit time for particles released on the same day.

215 3.3 Effect on river water concentrations

Given their effect on river water pathways and timescales, it is expected that tides would influence the river water concentrations over the shelf. As indicated in Figure 5, the water concentrations of the three rivers in the No-Tide case were approximately one order lower in magnitude than those in the Control run, especially in the Yellow and Bohai Seas. As against the Control run, when the tides were excluded, the annual mean river water concentrations of the Yellow, Yalujiang,
220 and Changjiang Rivers over the entire shelf were reduced by 73, 84, and 76 %, respectively. The mean reduction in the water

concentration of the three rivers in the Bohai and Yellow Seas is over 75 %, which is several times more than that in the East China Sea, suggesting that the tidal effect on river water concentrations is more significant in relatively enclosed seas than in relatively open seas.

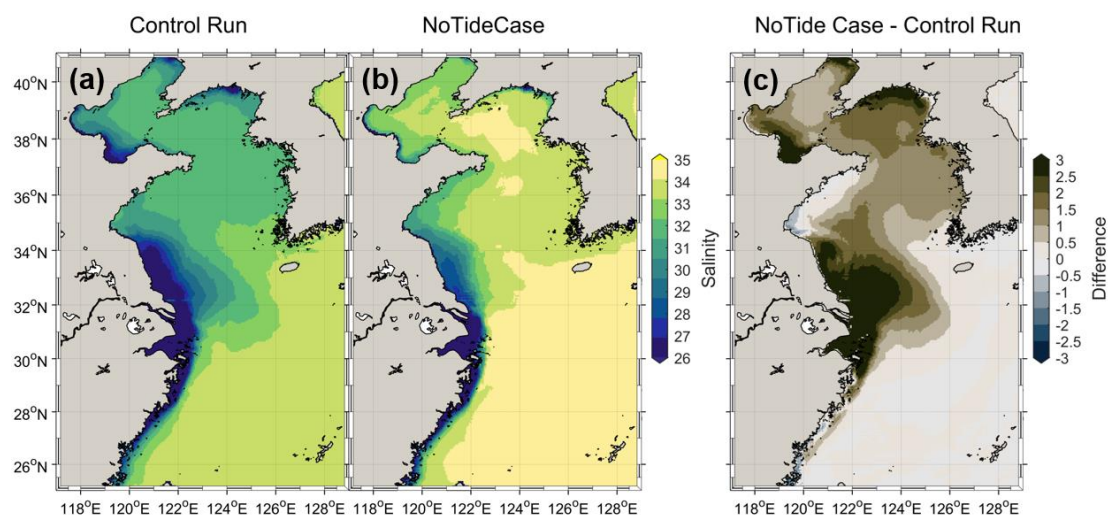


225 **Figure 5. The annually and vertically averaged river water concentrations of the three rivers for the Control run (a–c) and No-Tide case (d–f) (The maps show the logarithmic distribution of the obtained river water concentrations).**

A change in river water concentration can directly induce a change in seawater salinity over the shelf. As shown in Figure 6, the salinity in the estuaries and coastal waters is lower than 30 because of the input of freshwater from the rivers, while the salinity in the East China Sea is relatively high (>33) because of the salty water input from the Kuroshio Current (Figure 6a).
230 The seawater salinity in the No-Tide case increased significantly as against the Control run, particularly in the areas adjacent to the estuaries and in the Bohai and Yellow Seas (Figures 6b and 6c). This can be understood as the faster export of the



river water in the No-Tide case (Figures 3 and 4) leaving a smaller proportion of river freshwater in the shelf sea (Figure 5) and resulting in higher salinity over the shelf. The increase in salinity was more than 3 in the estuaries of the Yellow, 235 Yalujiang, and Changjiang Rivers and more than 1 (on average) in the Yellow and Bohai Seas (Figure 6c), while in the East China Sea, the magnitude of salinity change was smaller than 0.5, suggesting that the tidal effect on seawater salinity is more significant in relatively enclosed seas than in relatively open seas.



240 **Figure 6.** The annually and vertically averaged salinity of the shelf water for the Control run (a), No-Tide case (b), and their difference (c). Positive (negative) values denote the salinity of the No-Tide case as being higher (lower) than that of the Control run.

4 Discussion

4.1 Role of tidally induced change in the mixing and advection on the river water behavior

Changes in the river water transport pathways and timescales, and thus the river water concentrations and seawater salinity 245 in the shelf seas, indicate a significant effect of tides on the behavior of the river water over the shelf. The river water behavior over the shelf is determined by two processes, namely, advection and mixing. Tides can affect shelf current and water mixing and thus, influence river water transport over the shelf (Moon et al., 2009; Palma et al., 2004; Lin et al., 2020; Wang et al., 2013; Wu et al., 2018). To assess the respective effects of the changes in mixing and currents, induced by tides on river water transport, we designed two additional numerical experiments similar to the No-Tide case, except that in one, 250 the diffusivity coefficients driving the particle-tracking and passive tracer models were replaced by those in the Control run (hereafter termed “Tidal-Mixing case”), and in the other, the velocity and sea level driving the particle-tracking and tracer transport models were replaced by those in the Control run (hereafter termed “Tidal-Advection case”). The effect of the



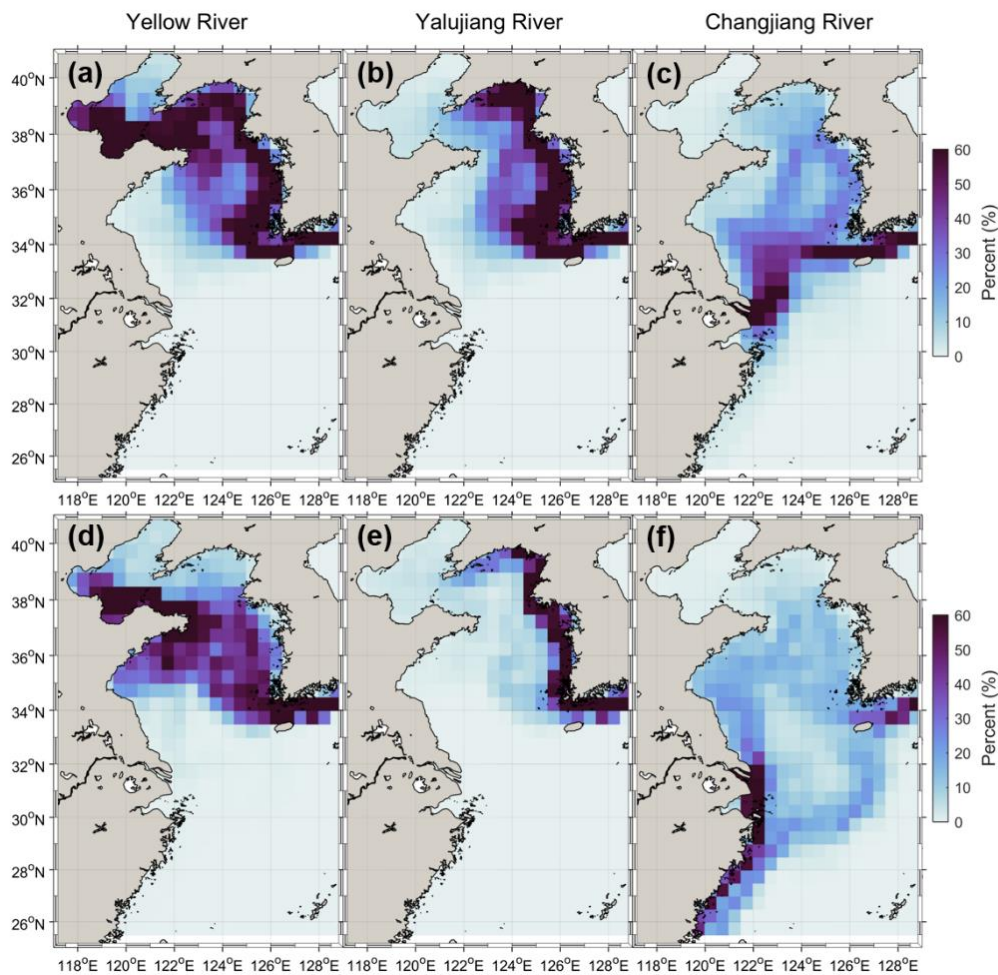
tidally induced change in the mixing and current on river water transport could be identified by comparing the results of the Tidal-Advection and Tidal-Mixing cases with those of the No-Tide case and Control run.

255 The river water transport pathways in the Tidal-Advection and Tidal-Mixing cases show a similar result to that in the Control run and No-Tide case, respectively (Figure 7), suggesting that tidally induced changes in the shelf currents are more important than those induced by water mixing for the river water pathways in the shelf sea. This is reasonable because the currents usually dominate horizontal transport, whereas mixing influences vertical transport.

For the transport timescales, the water age of the Tidal-Advection case was much higher than that of the No-Tide case and even higher than that of the Control run, whereas the water age of the Tidal-Mixing case was slightly lower than that of the No-Tide case (Figure 8). Similar to the results of the water age, the annual mean transit times of the Tidal-Mixing case were 2.4, 0.65, and 1.0 years for the Yellow, Yalujiang, and Changjiang Rivers, respectively, which are very close to the results of the No-Tide case (Figure 9); however, the transit time of the Tidal-Advection case was much higher than that of the No-Tide case. The water age and transit time results suggest that the tidally induced changes in currents and mixing had opposite

260 effects on the river water transport timescale, which decreased and increased the river water transport rate, respectively. As the transport timescales of the Control run (with tides) were much higher than those of the No-Tide case, we can infer that

265 the change in shelf currents induced by tides plays a dominant role in the transport rate of river water over the shelf.



270 **Figure 7.** The annually averaged water transport pathways of the three rivers over the shelf for the Tidal-Advection case (a–c) and Tidal-Mixing case (d–f), indicated by the emergence probability of the particles in the grids (in percent).

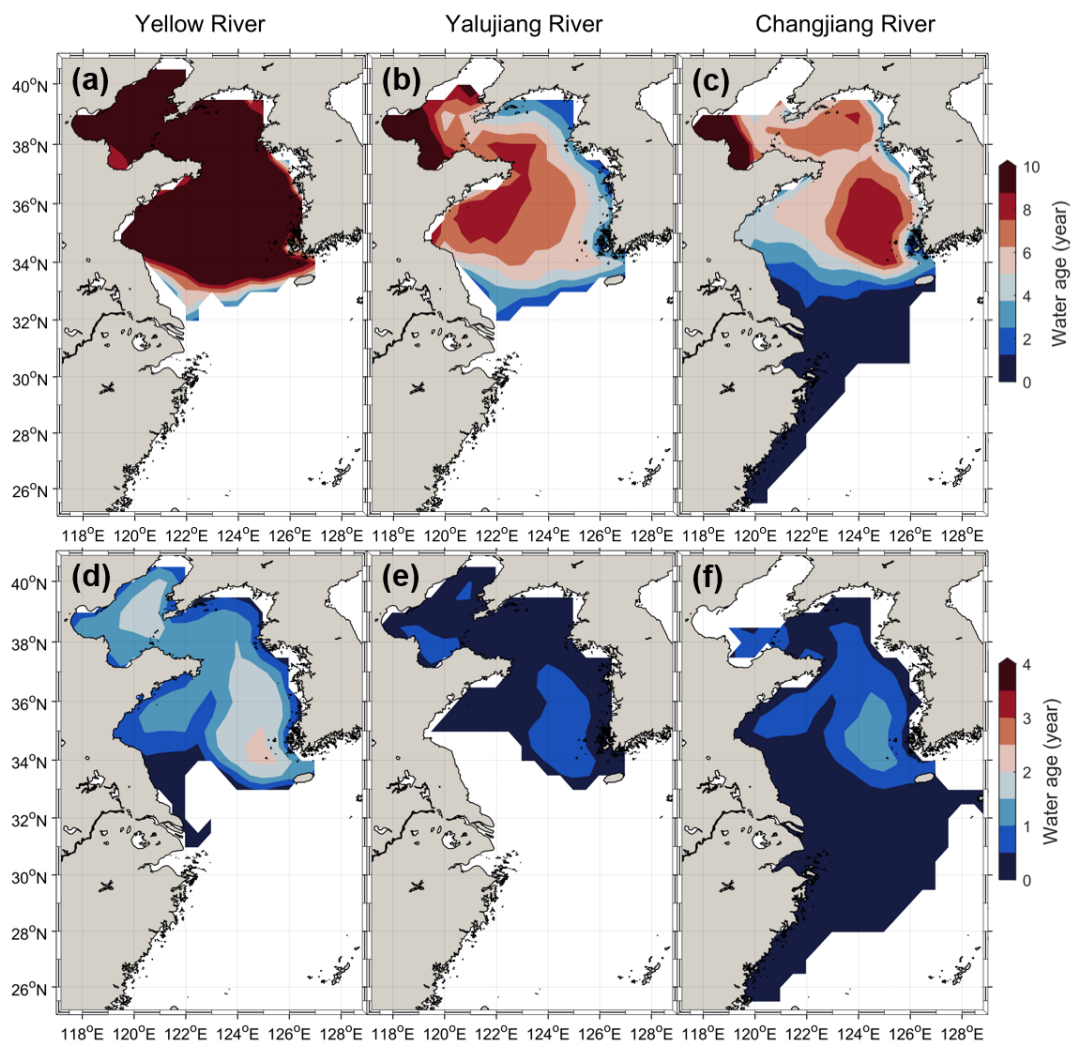
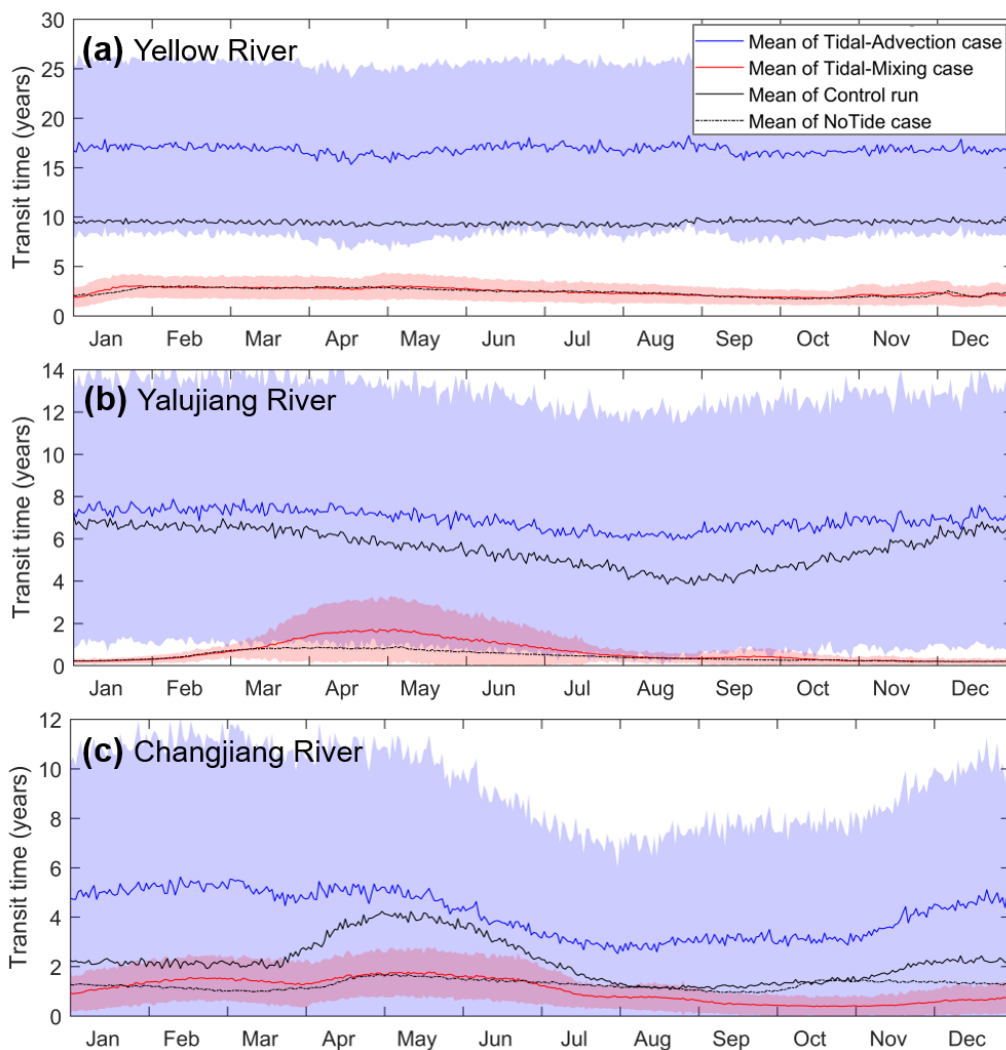


Figure 8. The annually and vertically averaged water age of the three rivers for the Tidal-Advection case (a–c) and Tidal-Mixing case (d–f).



275 **Figure 9.** The daily mean water transit time over the shelf of the three rivers for the Tidal-Advection case (blue) and Tidal-Mixing case (red), along with the Control run (black) and No-Tide case (dotted black).

4.2 Effect of tidally induced changes in the shelf current on river water transport

To further understand the effect of tidally induced changes in currents on river water transport, we compared and analyzed
280 the monthly mean shelf currents of the Control run and the No-Tide case (Figure 10). The shelf currents for the Control run were much weaker than those for the No-Tide case, especially in the coastal areas and the Bohai and Yellow Seas during winter. During winter, the coastal currents along the Jiangsu and the west Korea in the No-Tide case were several times stronger as against those in the Control run. The Yellow Sea Warm Current was also significantly strengthened in the model



without tides (Figure 10b). Lin et al., (2020) has well explained the cause of the difference in the intensify of the shelf
285 circulation between the No-Tide case and the Control run and suggested the important role of the tidally induced change in
bottom friction. In a model with tides, bottom resistance is intensified, thus decreasing coastal wind-driven currents. The
decrease in coastal currents results in a smaller gradient of sea surface height across the continental shelf, and thus
weakening Yellow Sea Warm Current in winter in the Control run compared to the No-Tide case. Moreover, tides can
induce tidal residual currents and modulate shelf currents, which could be important for the tidal effect on coastal currents
290 during the summer (Lie and Cho, 2016; Moon et al., 2009). In the East China Sea, there is no obvious difference in the shelf
currents between the Control run and No-Tide Case because of the dominant role of the outer shelf currents (the Kuroshio
Current and the Taiwan Warm Current) in the shelf circulation. On the other hand, the relatively deep water depths of the
East China Sea (averaging about 80 m) are less influenced by changes in bottom friction on shelf currents than the relatively
shallow Yellow Sea (averaging about 40 m) and Bohai Sea (averaging about 20 m). Thus, the effect of tides on river water
295 behavior in the East China Sea were relatively smaller than those in the Yellow and Bohai seas.

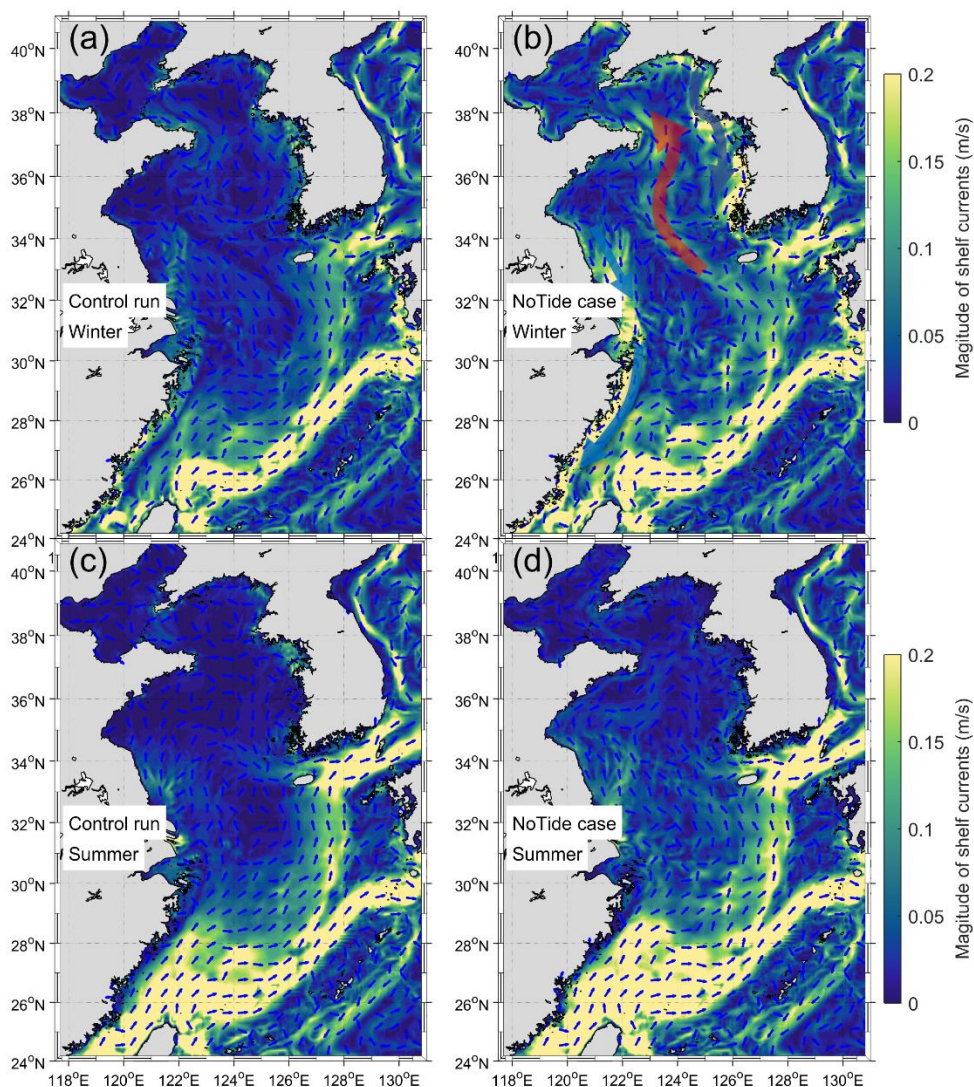


Figure 10. Monthly and vertically averaged velocity for the Control run (left panels) and No-Tide case (right panels), respectively. (a, c) for February and (b, d) for August. The red arrow in (b) denotes the intensified Yellow Sea Warm Current during winter in the No-Tide case. The blue arrows in (b) denote the intensified coastal currents.

300

For the Yellow and Yalujiang Rivers, the significantly intensified coastal currents in the Yellow and Bohai Seas in the No-Tide case accelerated water transport along the coasts to the Cheju Strait and induced much smaller transport timescales than those of the Control run. Meanwhile, the pathways of the Yalujiang and Yellow Rivers water were more dispersed in the Control run than the No-Tide case (Figures 2d and 2e), given that, the tidal dispersion in the coastal region could intensify the dispersion during the river water transport process (Zimmerman et al. 1986; Geyer et al., 1992) and increase the transit

305



area of the Yellow and Yalujiang Rivers. However, for the Changjiang River water, the main pathways in the Control run were northeastward, as far as the Tsushima Strait (Figure 2c). In the No-Tide case, the strengthened Jiangsu and Zhejiang coastal currents transported more Changjiang River water to the Jiangsu and Zhejiang coasts, and the strengthened Yellow Sea Warm Current transported more river water to the Yellow Sea. This could explain why the transport pathways of the Changjiang River water were more dispersed in the No-Tide case than in the Control run (Figure 2f). The enhanced coastal currents and shelf circulations of the No-Tide case can accelerate river water transport over the shelf and thus induce much shorter water transport timescales in the Changjiang River.

4.3 Whether a tidal parameterization can improve the simulation in a no-tide model?

The present study shows that tides could have a significant effect on river water transport, concentration, and seawater salinity in shelf seas by changing the bottom resistance and reducing the shelf currents. Tidal parameterization can include the tidal effect on hydrodynamics in a no-tide model to some extent. To examine the availability of tidal parameterization in no-tide models for the simulation of river water transport on the shelf, we added a parameterized-tide experiment (PMT-Tide case), wherein, linear-type bottom friction considering the tidal effect proposed by Lee et al. (2000) was applied to the hydrodynamic model. The method has been used in studies on the shelf currents in the Yellow Sea and ESSC (Moon et al., 2009; Lin et al., 2020). The details of the parameterization were presented by Moon et al. (2009) and Lin et al. (2020). Then, using the hydrodynamic forcing of the parameterized-tide model, the water transport pathways and timescales, and the water concentrations of the rivers in the ESSC were diagnosed using the same procedures described in Sections 2.3 and 2.4.

The experimental results showed that the tidal parameterization could not significantly improve the simulation of the river water transport pathways and the pattern of the river water age over the shelf. As compared with the Control run, the river water pathways of the Yellow and Yalujiang Rivers in the PMT-Tide case were still very concentrated in the coastal region, and that of the Changjiang River was more dispersed in the Yellow Sea (Figure 11). The transit time of the Yellow River for the PMT-Tide case was close to the result of the Control run (~0.2 years bias), while those of the Yalujiang and Changjiang Rivers still showed a large bias (more than 3.4 years) as compared to the Control run (Figure 12). When compared with the No-Tide case, the PMT-Tide case could increase the water concentration of the Yellow and Changjiang Rivers (Figure 11) and thus improve the simulation of salinity over the shelf to some extent; however, there was still a large bias in the simulated salinity (> 3) in the estuarine zones (Figure 13). Therefore, the tidal parameterization in a no-tide model could not adequately consider the effect of tides on river water transport, implying that a better tidal parameterization for no-tide ocean models needs further development and examination in future work, or explicitly considering the tides in ocean models is necessary.

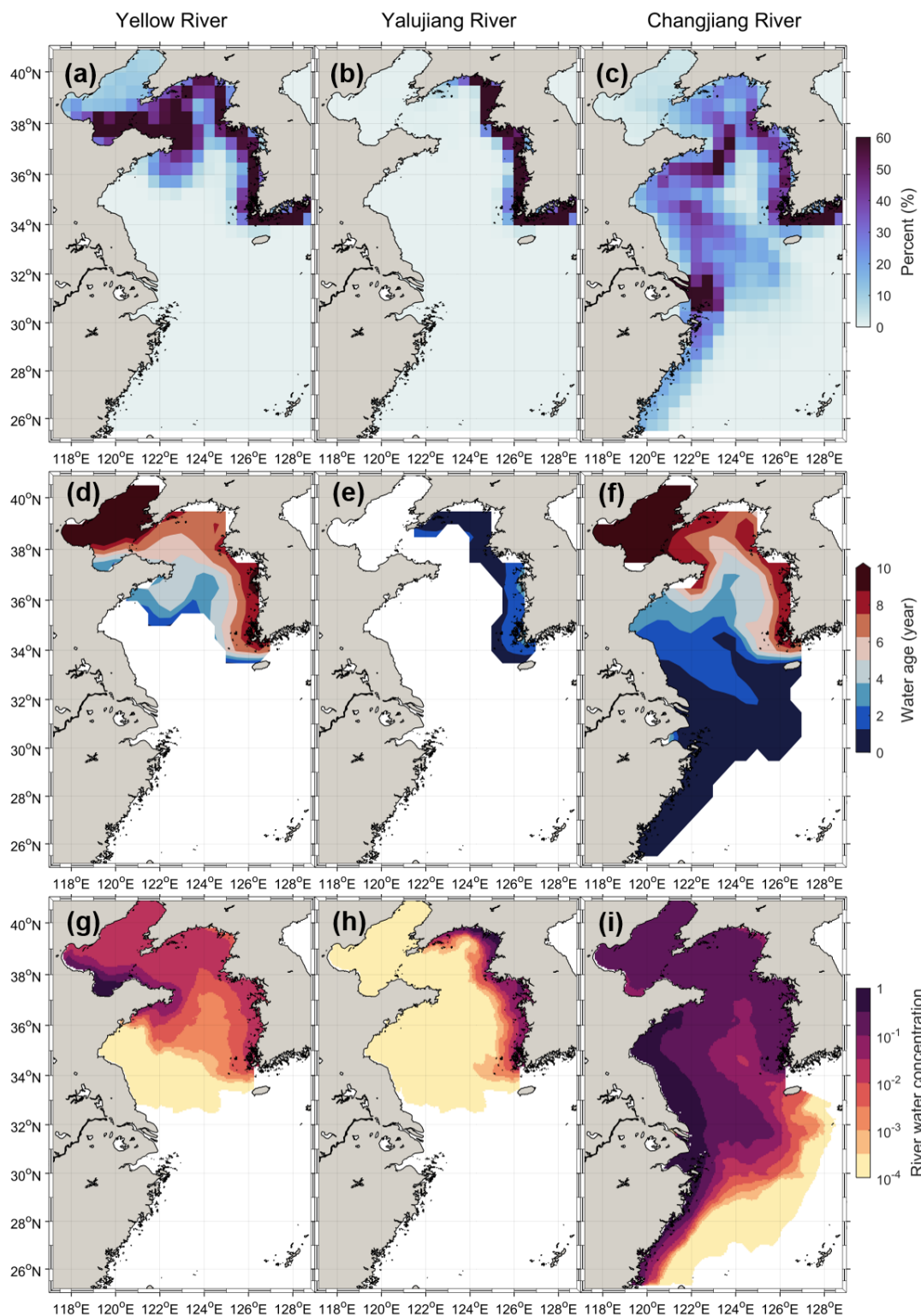
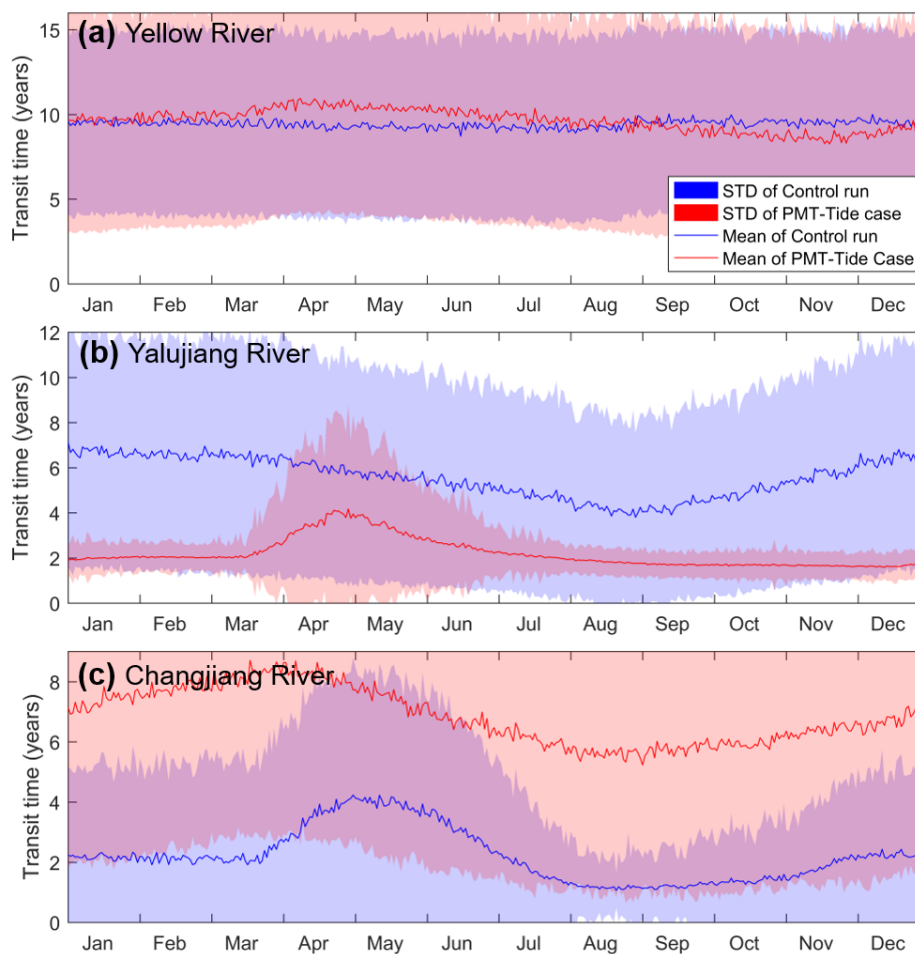


Figure 11. The three rivers' waters transport pathways, age, and concentration for the PMT-Tide case. The annually averaged emerging probability of particles (a–c). The annually and vertically averaged water age (d–f). The annually and vertically averaged river water concentration (g–i).



340 **Figure 12.** The daily mean water transit time over the shelf of the three rivers for the Control run (blue) and PMT-Tide case (red). STD in the figure label denotes the standard deviation of the transit time for particles released on the same day.

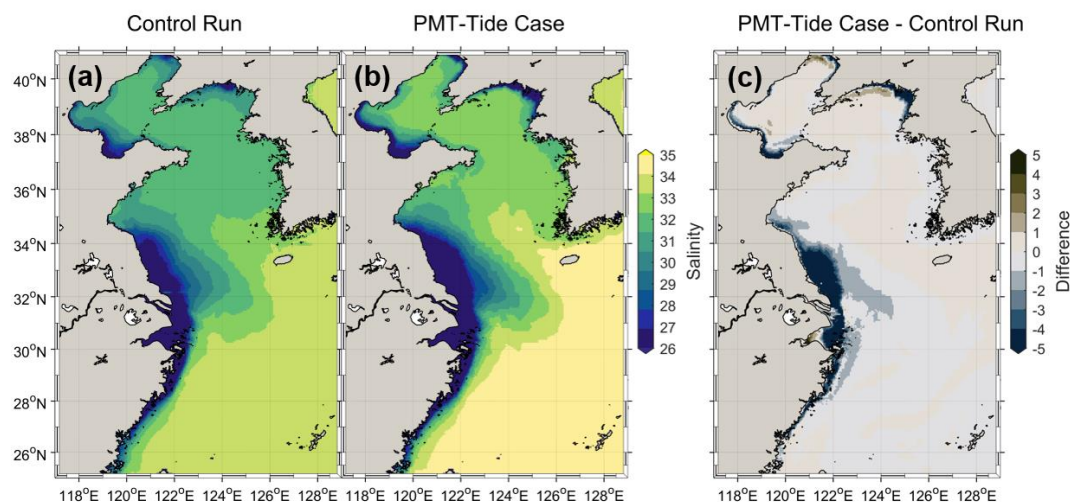


Figure 13. The annually and vertically averaged salinity of the shelf water for the Control run (a), the PMT-Tide case (b), and their difference (c). Positive (negative) values denote the salinity of the No-Tide case higher (lower) than that of the Control run.

345 4.4 Implications on climate modeling

The present study demonstrated that tides have a significant effect on river water transport pathways, timescales, river water concentration, and shelf seawater salinity. Moreover, the improvement of tidal parameterization in the simulation of a no-tide model could be very limited. Therefore, if earth system models or climate models do not explicitly considered tides, the model results will have a large bias in the river water transport process over shelf seas. Consequently, such biases may seriously affect the accuracy of global model predictions of global water and carbon cycles and even climate change for the following reasons. First, river runoff which accounts for about 10% of the global meridional water fluxes play a significant role in the ocean circulation through affecting the water balance and salinity of the oceans (Oki et al., 1995; 1999). The absence of tides in global models could accelerate the freshwater export from shelf seas to deep oceans and influence the salinity balance and circulations in oceans. Second, river water is rich in terrigenous nutrients, which are an important source of nutrients for phytoplankton in shelf seas. Shelf seas contribute to approximately 1/3 of the marine primary productivity and 40 % of the ocean carbon storage, and the carbon pumping of shelf seas is an important way of global carbon sequestration, thus shelf seas playing a critical role in the global carbon cycle (Thomas, 2004; Laruelle et al., 2018; Dunne et al., 2007). The absence of tides will change the nutrient transport pathways and timescales and reduce the concentration of terrigenous nutrients, which will directly change the primary productivity of shelf seas. Meanwhile, the absence of tides significantly increased the seawater salinity of the shelf seas. The total alkalinity of seawater is controlled mainly by salinity (Millero et al., 1998), dominating the air-sea CO₂ flux (Kantha, 2004). Thus, the change in primary productivity and the bias in seawater salinity could ultimately lead to errors in the simulation of the CO₂ flux and carbon cycle in shelf seas in climate models. Third, the terrigenous organic and inorganic carbon carried by rivers is over 0.8 PgC/year (1 Pg = 10¹⁵ g) and is input into shelf seas (Bauer et al., 2013). The simulation of the export rate of river water and terrigenous carbon in shelf seas



365 in a no-tide model would be falsely accelerated, which may reduce terrigenous carbon burial and emission in the shelf sea
and thus increase the amount of terrigenous carbon entering the open ocean (Schlünz & Schneider, 2000). In these ways, the
absence of tides in climate models could induce a strong uncertainty in the simulation of the carbon cycle and thus affect the
accuracy of the climate projection of the climate models and the earth system models. However, the effect of the change of
the river water behavior in no-tide models on the bias of the carbon cycle simulation and climate projection still need to be
370 further quantitatively studied using a high-resolution earth system model.

5 Conclusions

Using numerical modeling and sensitivity experiments, this study assessed the effect of tides on river water transport
pathways and timescales and the water concentration of three major rivers (i.e., the Yellow, Yalujiang, and Changjiang
Rivers) in the ESSC. The model results suggest that tides induced more dispersed transport pathways for the Yellow and
375 Yalujiang Rivers, but more concentrated transport pathways for the Changjiang River. By weakening the shelf currents, tides
increased the water transport timescales of the three rivers by 2–10 times and thus significantly slowed the transport and
export of the river water over the shelf. The slow export of river water induced by tides increased the river water
concentration by approximately one order in magnitude and decreased seawater salinity in the ESSC. Moreover, the effects
of tides on river water behavior was stronger in relatively enclosed seas (i.e., the Bohai and Yellow Seas) than in relatively
380 open seas (i.e., the East China Sea). Given the important role of river water in water and carbon cycling, climate and earth
system models without tides may be biased in simulating and predicting the global water and carbon cycle. Therefore, the
effects of tides on river water behavior should be carefully considered in climate and earth system modeling.

Code availability

385 The source code of numerical model used in this study is available on request. Please contact Lei Lin (llin@sdust.edu.cn).

Data availability

The model data are shown in the figures in the main text which is available on request. Please contact Lei Lin
(llin@sdust.edu.cn).



Author contributions

390 LL, HL, and QF conducted the numerical experiments and analyzed the data. LL, HL, and XH wrote the initial draft, and all authors have contributed to editing the paper. XG provided the hydrodynamic model. All authors contributed to discussing and interpreting the results.

Competing interests

The contact author has declared that neither they nor their co-authors have any competing interests.

395 Acknowledgments

This study was supported by the National Key Research and Development Program of China(2020YFA0607900) and the National Natural Science Foundation of China (Grant No. 41706011). Xinyu Guo was supported by Grants-in-Aid for Scientific Research (MEXT KAKENHI grant numbers: 20H04319).

References

- 400 Bauer, J. E., Cai, W.-J., Raymond, P. A., Bianchi, T. S., Hopkinson, C. S., and Regnier, P. A. G.: The changing carbon cycle of the coastal ocean, *Nature*, 504, 61–70, <https://doi.org/10.1038/nature12857>, 2013.
- Blumberg, A. F. (2002), A primer for ECOMSED user manual [version 1.3], technical report, HydroQual, Mahwah, N. J.
- Blumberg, A. F. and Mellor, G. L.: A Description of a Three-Dimensional Coastal Ocean Circulation Model, in: Three-Dimensional Coastal Ocean Models, American Geophysical Union (AGU), 1–16, <https://doi.org/10.1029/CO004p0001>,
405 1987.
- Brady, E., Stevenson, S., Bailey, D., Liu, Z., Noone, D., Nusbaumer, J., Otto-Bliesner, B. L., Tabor, C., Tomas, R., Wong, T., Zhang, J., and Zhu, J.: The Connected Isotopic Water Cycle in the Community Earth System Model Version 1, *J ADV MODEL EARTH SY*, 11, 2547–2566, <https://doi.org/10.1029/2019MS001663>, 2019.
- Clark, M. P., Fan, Y., Lawrence, D. M., Adam, J. C., Bolster, D., Gochis, D. J., Hooper, R. P., Kumar, M., Leung, L. R.,
410 Mackay, D. S., Maxwell, R. M., Shen, C., Swenson, S. C., and Zeng, X.: Improving the representation of hydrologic processes in Earth System Models, *WATER RESOUR RES*, 51, 5929–5956, <https://doi.org/10.1002/2015WR017096>, 2015.
- Deleersnijder, E., Campin, J.-M., and Delhez, E. J. M.: The concept of age in marine modelling: I. Theory and preliminary model results, *J MARINE SYST*, 28, 229–267, [https://doi.org/10.1016/S0924-7963\(01\)00026-4](https://doi.org/10.1016/S0924-7963(01)00026-4), 2001.
- Ding, X., Guo, X., Zhang, C., Yao, X., Liu, S., Shi, J., Luo, C., Yu, X., Yu, Y., and Gao, H.: Water conservancy project on
415 the Yellow River modifies the seasonal variation of Chlorophyll-a in the Bohai Sea, *CHEMOSPHERE*, 254, 126846, <https://doi.org/10.1016/j.chemosphere.2020.126846>, 2020.



- Dittmar, T. and Kattner, G.: The biogeochemistry of the river and shelf ecosystem of the Arctic Ocean: a review, *Marine Chemistry*, 83, 103–120, [https://doi.org/10.1016/S0304-4203\(03\)00105-1](https://doi.org/10.1016/S0304-4203(03)00105-1), 2003.
- Dufresne, J.-L., Foujols, M.-A., Denvil, S., Caubel, A., Marti, O., Aumont, O., Balkanski, Y., Bekki, S., Bellenger, H.,
420 Benschila, R., Bony, S., Bopp, L., Braconnot, P., Brockmann, P., Cadule, P., Cheruy, F., Codron, F., Cozic, A., Cugnet, D., de
Noblet, N., Duvel, J.-P., Ethé, C., Fairhead, L., Fichet, T., Flavoni, S., Friedlingstein, P., Grandpeix, J.-Y., Guez, L.,
Guilyardi, E., Hauglustaine, D., Hourdin, F., Idelkadi, A., Ghattas, J., Joussaume, S., Kageyama, M., Krinner, G., Labetoulle,
S., Lahellec, A., Lefebvre, M.-P., Lefevre, F., Levy, C., Li, Z. X., Lloyd, J., Lott, F., Madec, G., Mancip, M., Marchand, M.,
Masson, S., Meurdesoif, Y., Mignot, J., Musat, I., Parouty, S., Polcher, J., Rio, C., Schulz, M., Swingedouw, D., Szopa, S.,
425 Talandier, C., Terray, P., Viovy, N., and Vuichard, N.: Climate change projections using the IPSL-CM5 Earth System Model:
from CMIP3 to CMIP5, *Clim Dyn*, 40, 2123–2165, <https://doi.org/10.1007/s00382-012-1636-1>, 2013.
- Dunne, J. P., Sarmiento, J. L., and Gnanadesikan, A.: A synthesis of global particle export from the surface ocean and
cycling through the ocean interior and on the seafloor, *GLOBAL BIOGEOCHEM CY*, 21,
<https://doi.org/10.1029/2006GB002907>, 2007.
- 430 Feng, Y., Menemenlis, D., Xue, H., Zhang, H., Carroll, D., Du, Y., and Wu, H.: Improved representation of river runoff in
Estimating the Circulation and Climate of the Ocean Version 4 (ECCOV4) simulations: implementation, evaluation, and
impacts to coastal plume regions, *Geosci Model Dev*, 14, 1801–1819, <https://doi.org/10.5194/gmd-14-1801-2021>, 2021.
- Geyer, W. R. and Signell, R. P.: A Reassessment of the Role of Tidal Dispersion in Estuaries and Bays, *Estuaries*, 15, 97–
108, <https://doi.org/10.2307/1352684>, 1992.
- 435 Gong, G.-C., Liu, K.-K., Chiang, K.-P., Hsiung, T.-M., Chang, J., Chen, C.-C., Hung, C.-C., Chou, W.-C., Chung, C.-C.,
Chen, H.-Y., Shiah, F.-K., Tsai, A.-Y., Hsieh, C., Shiao, J.-C., Tseng, C.-M., Hsu, S.-C., Lee, H.-J., Lee, M.-A., Lin, I.-I.,
and Tsai, F.: Yangtze River floods enhance coastal ocean phytoplankton biomass and potential fish production, *GEOPHYS
RES LETT*, 38, <https://doi.org/10.1029/2011GL047519>, 2011.
- Graham, J. A., Rosser, J. P., O’Dea, E., and Hewitt, H. T.: Resolving Shelf Break Exchange Around the European Northwest
440 Shelf, *GEOPHYS RES LETT*, 45, 12,386–12,395, <https://doi.org/10.1029/2018GL079399>, 2018.
- Guo, X. and Valle-Levinson, A.: Tidal effects on estuarine circulation and outflow plume in the Chesapeake Bay, *CONT
SHELF RES*, 27, 20–42, <https://doi.org/10.1016/j.csr.2006.08.009>, 2007.
- Guo, X. and Yanagi, T.: Three-dimensional structure of tidal current in the East China Sea and the Yellow Sea, *J
OCEANOGR*, 54, 651–668, <https://doi.org/10.1007/BF02823285>, 1998.
- 445 Guo, X., Hukuda, H., Miyazawa, Y., and Yamagata, T.: A Triply Nested Ocean Model for Simulating the Kuroshio—Roles
of Horizontal Resolution on JEBAR, *J PHYS OCEANOGR*, 33, 146–169, [https://doi.org/10.1175/1520-0485\(2003\)033<0146:ATNOMF>2.0.CO;2](https://doi.org/10.1175/1520-0485(2003)033<0146:ATNOMF>2.0.CO;2), 2003.
- Guo, X., Miyazawa, Y., and Yamagata, T.: The Kuroshio Onshore Intrusion along the Shelf Break of the East China Sea:
The Origin of the Tsushima Warm Current, *J PHYS OCEANOGR*, 36, 2205–2231, <https://doi.org/10.1175/JPO2976.1>, 2006.



- 450 Holt, J., Hyder, P., Ashworth, M., Harle, J., Hewitt, H. T., Liu, H., New, A. L., Pickles, S., Porter, A., Popova, E., Allen, J. I., Siddorn, J., and Wood, R.: Prospects for improving the representation of coastal and shelf seas in global ocean models, *GEOSCI MODEL DEV*, 10, 499–523, <https://doi.org/10.5194/gmd-10-499-2017>, 2017.
- Hopkinson, C. S. and Vallino, J. J.: Efficient export of carbon to the deep ocean through dissolved organic matter, *Nature*, 433, 142–145, <https://doi.org/10.1038/nature03191>, 2005.
- 455 Kantha, L. H.: A general ecosystem model for applications to primary productivity and carbon cycle studies in the global oceans, *OCEAN MODEL*, 6, 285–334, [https://doi.org/10.1016/S1463-5003\(03\)00022-2](https://doi.org/10.1016/S1463-5003(03)00022-2), 2004.
- Laruelle, G. G., Cai, W.-J., Hu, X., Gruber, N., Mackenzie, F. T., and Regnier, P.: Continental shelves as a variable but increasing global sink for atmospheric carbon dioxide, *NAT COMMUN*, 9, 454, <https://doi.org/10.1038/s41467-017-02738-z>, 2018.
- 460 Lee, H. J., Jung, K. T., Foreman, M. G. G., and Chung, J. Y.: A three-dimensional mixed finite-difference Galerkin function model for the oceanic circulation in the Yellow Sea and the East China Sea, *CONT SHELF RES*, 20, 863–895, [https://doi.org/10.1016/S0278-4343\(00\)00005-4](https://doi.org/10.1016/S0278-4343(00)00005-4), 2000.
- Lee, H.-C., Rosati, A., and Spelman, M. J.: Barotropic tidal mixing effects in a coupled climate model: Oceanic conditions in the Northern Atlantic, *OCEAN MODEL*, 11, 464–477, <https://doi.org/10.1016/j.ocemod.2005.03.003>, 2006.
- 465 Lie, H.-J. and Cho, C.-H.: Seasonal circulation patterns of the Yellow and East China Seas derived from satellite-tracked drifter trajectories and hydrographic observations, *PROG OCEANOGR*, 146, 121–141, <https://doi.org/10.1016/j.pocean.2016.06.004>, 2016.
- Lin, L. and Liu, Z.: Partial residence times: determining residence time composition in different subregions, *OCEAN DYNAM*, 69, 1023–1036, <https://doi.org/10.1007/s10236-019-01298-8>, 2019a.
- 470 Lin, L. and Liu, Z.: TVDal: Total variation diminishing scheme with alternating limiters to balance numerical compression and diffusion, *OCEAN MODEL*, 134, 42–50, <https://doi.org/10.1016/j.ocemod.2019.01.002>, 2019b.
- Lin, L., Liu, D., Guo, X., Luo, C., and Cheng, Y.: Tidal Effect on Water Export Rate in the Eastern Shelf Seas of China, *J GEOPHYS RES-OCEANS*, 125, e2019JC015863, <https://doi.org/10.1029/2019JC015863>, 2020.
- Liu, K., Atkinson, L., Quinones, R., and Talaue-McManus, L.: Carbon and Nutrient Fluxes in Continental Margins: A
475 Global Synthesis, Springer Nature, 772 pp., 2010.
- Liu, Z., Lin, L., Xie, L., and Gao, H.: Partially implicit finite difference scheme for calculating dynamic pressure in a terrain-following coordinate non-hydrostatic ocean model, *OCEAN MODEL*, 106, 44–57, <https://doi.org/10.1016/j.ocemod.2016.09.004>, 2016.
- Liu, Z., Wang, H., Guo, X., Wang, Q., and Gao, H.: The age of Yellow River water in the Bohai Sea, *J GEOPHYS RES-OCEANS*, 117, 317–323, <https://doi.org/10.1029/2012JC008263>, 2012.
- 480 Luneva, M. V., Aksenov, Y., Harle, J. D., and Holt, J. T.: The effects of tides on the water mass mixing and sea ice in the Arctic Ocean, *J GEOPHYS RES-OCEANS*, 120, 6669–6699, <https://doi.org/10.1002/2014JC010310>, 2015.



- Mackenzie, F. T., Ver, L. M., and Lerman, A.: Century-scale nitrogen and phosphorus controls of the carbon cycle, *CHEM GEOL*, 190, 13–32, [https://doi.org/10.1016/S0009-2541\(02\)00108-0](https://doi.org/10.1016/S0009-2541(02)00108-0), 2002.
- 485 Mellor, G. L.: Users guide for a three dimensional, primitive equation, numerical ocean model, Program in Atmospheric and Oceanic Sciences, Princeton University Princeton, NJ 08544-0710, 56 pp., 1998.
- Millero, F. J., Lee, K., and Roche, M.: Distribution of alkalinity in the surface waters of the major oceans, *MAR CHEM*, 60, 111–130, [https://doi.org/10.1016/S0304-4203\(97\)00084-4](https://doi.org/10.1016/S0304-4203(97)00084-4), 1998.
- Moon, J. H., Hirose, N., and Yoon, J. H.: Comparison of wind and tidal contributions to seasonal circulation of the Yellow
490 Sea, *J GEOPHYS RES-OCEANS*, 114, <https://doi.org/10.1029/2009JC005314>, 2009.
- Müller, M., Haak, H., Jungclaus, J. H., Sündermann, J., and Thomas, M.: The effect of ocean tides on a climate model simulation, *OCEAN MODEL*, 35, 304–313, <https://doi.org/10.1016/j.ocemod.2010.09.001>, 2010.
- Oki, T., Entekhabi, D., & Harrold, T. I. (1999). The global water cycle. *Global energy and water cycles*, 10, 27, 1999.
- Oki, T., Musiaka, K., Matsuyama, H., and Masuda, K.: Global atmospheric water balance and runoff from large river basins,
495 *Hydrol Process*, 9, 655–678, <https://doi.org/10.1002/hyp.3360090513>, 1995.
- Palma, E. D., Matano, R. P., and Piola, A. R.: A numerical study of the Southwestern Atlantic Shelf circulation: Barotropic response to tidal and wind forcing, *J GEOPHYS RES-OCEANS*, 109, <https://doi.org/10.1029/2004JC002315>, 2004.
- Schlünz, B. and Schneider, R.: Transport of terrestrial organic carbon to the oceans by rivers: Re-estimating flux- and burial rates, *INT J EARTH SCI*, 88, 599–606, <https://doi.org/10.1007/s005310050290>, 2000.
- 500 Simmons, H. L., Jayne, S. R., Laurent, L. C. St., and Weaver, A. J.: Tidally driven mixing in a numerical model of the ocean general circulation, *OCEAN MODEL*, 6, 245–263, [https://doi.org/10.1016/S1463-5003\(03\)00011-8](https://doi.org/10.1016/S1463-5003(03)00011-8), 2004.
- Tang, Q., Huang, X., Lin, L., Xiong, W., Wang, D., Wang, M., and Huang, X.: MERF v3.0, a highly computationally efficient non-hydrostatic ocean model with implicit parallelism: Algorithms and validation experiments, *OCEAN MODEL*, 167, 101877, <https://doi.org/10.1016/j.ocemod.2021.101877>, 2021.
- 505 Thomas, H.: Enhanced Open Ocean Storage of CO₂ from Shelf Sea Pumping, *Science*, 304, 1005–1008, <https://doi.org/10.1126/science.1095491>, 2004.
- Voldoire, A., Sanchez-Gomez, E., Salas Y Mélia, D., Decharme, B., Cassou, C., Sénési, S., Valcke, S., Beau, I., Alias, A., Chevallier, M., Déqué, M., Deshayes, J., Douville, H., Fernandez, E., Madec, G., Maisonnave, E., Moine, M. P., Planton, S., Saint-Martin, D., Szopa, S., Tyteca, S., Alkama, R., Belamari, S., Braun, A., Coquart, L., and Chauvin, F.: The CNRM-
510 CM5.1 global climate model: description and basic evaluation, *CLIM DYNAM*, 40, 2091–2121, <https://doi.org/10.1007/s00382-011-1259-y>, 2013.
- Wang, Q., Guo, X., and Takeoka, H.: Seasonal variations of the Yellow River plume in the Bohai Sea: A model study, *J GEOPHYS RES-OCEANS*, 113, <https://doi.org/10.1029/2007JC004555>, 2008.
- Wang, Q.: Enhanced cross-shelf exchange by tides in the western Ross Sea. *Geophysical Research Letters*, 40(21), 5587-
515 5591., *GEOPHYS RES LETT*, 40, 5587–5591, <https://doi.org/10.1002/2013GL058258>, 2013.



- Wang, Y., Guo, X., Zhao, L., and Zhang, J.: Seasonal variations in nutrients and biogenic particles in the upper and lower layers of East China Sea Shelf and their export to adjacent seas, *PROG OCEANOGR*, 176, 102138, <https://doi.org/10.1016/j.pocean.2019.102138>, 2019.
- Winkelbauer, S., Mayer, M., Seitner, V., Zsoter, E., Zuo, H., and Haimberger, L.: Diagnostic evaluation of river discharge into the Arctic Ocean and its impact on oceanic volume transports, *Hydrol Earth Syst Sci*, 26, 279–304, <https://doi.org/10.5194/hess-26-279-2022>, 2022.
- Wu, H., Gu, J., and Zhu, P.: Winter Counter-Wind Transport in the Inner Southwestern Yellow Sea, *J GEOPHYS RES-OCEANS*, 123, 411–436, <https://doi.org/10.1002/2017JC013403>, 2018.
- Wu, H., Shen, J., Zhu, J., Zhang, J., and Li, L.: Characteristics of the Changjiang plume and its extension along the Jiangsu Coast, *CONT SHELF RES*, 76, 108–123, <https://doi.org/10.1016/j.csr.2014.01.007>, 2014.
- Wu, H., Zhu, J., Shen, J., and Wang, H.: Tidal modulation on the Changjiang River plume in summer, *J GEOPHYS RES-OCEANS*, 116, <https://doi.org/10.1029/2011JC007209>, 2011.
- Wu, T. and Wu, H.: Tidal Mixing Sustains a Bottom-Trapped River Plume and Buoyant Coastal Current on an Energetic Continental Shelf, *J GEOPHYS RES-OCEANS*, 123, 8026–8051, <https://doi.org/10.1029/2018JC014105>, 2018.
- Yang, F., Wei, Q., Chen, H., and Yao, Q.: Long-term variations and influence factors of nutrients in the western North Yellow Sea, China, *MAR POLLUT BULL*, 135, 1026–1034, <https://doi.org/10.1016/j.marpolbul.2018.08.034>, 2018.
- Yu, X., Guo, X., and Gao, H.: Detachment of Low-Salinity Water From the Yellow River Plume in Summer, *J GEOPHYS RES-OCEANS*, 125, e2020JC016344, <https://doi.org/10.1029/2020JC016344>, 2020.
- Yu, X., Guo, X., Gao, H., and Zou, T.: Upstream Extension of a Bottom-Advected Plume and Its Mechanism: The Case of the Yellow River, *J PHYS OCEANOGR*, 51, 2351–2371, <https://doi.org/10.1175/JPO-D-20-0235.1>, 2021.
- Zhang, J., Guo, X., and Zhao, L.: Budget of riverine nitrogen over the East China Sea shelf, *ENVIRON POLLUT*, 289, 117915, <https://doi.org/10.1016/j.envpol.2021.117915>, 2021.
- Zhang, J., Guo, X., and Zhao, L.: Tracing external sources of nutrients in the East China Sea and evaluating their contributions to primary production, *PROG OCEANOGR*, 176, 102122, <https://doi.org/10.1016/j.pocean.2019.102122>, 2019.
- Zhao, L. and Guo, X.: Influence of cross-shelf water transport on nutrients and phytoplankton in the East China Sea: a model study, *OCEAN SCI*, 7, 27–43, <https://doi.org/10.5194/os-7-27-2011>, 2011.
- Zhu, J., Shi, J., Guo, X., Gao, H., and Yao, X.: Air-sea heat flux control on the Yellow Sea Cold Water Mass intensity and implications for its prediction, *CONT SHELF RES*, 152, 14–26, <https://doi.org/10.1016/j.csr.2017.10.006>, 2018.
- Zimmerman, J. T. F.: The tidal whirlpool: A review of horizontal dispersion by tidal and residual currents, *NETH J SEA RES*, 20, 133–154, [https://doi.org/10.1016/0077-7579\(86\)90037-2](https://doi.org/10.1016/0077-7579(86)90037-2), 1986.